THE COMPLEX, THREE-DIMENSIONAL MAGNETOPAUSE

F.S. Mozer, T.D. Phan, and S.D. Bale

Physics Department and Space Sciences Laboratory

University of California, Berkeley, CA. 94720

ABSTRACT

Electric and magnetic fields observed in a one-of-a-kind example of a Polar satellite magnetopause crossing[1] are consistent with static guide magnetic and electric fields, Hall MHD electric and magnetic fields, and a Z-component magnetic field that varied from –80 nT to +80 nT across the magnetopause. In spite of this excellent agreement with simulations, other features of the data were unanticipated. We develop an empirical model based on these measured fields and the assumption that the parallel electric field was zero, to explain such features by showing that:

1. Post-reconnection $\mathbf{E}\mathrm{X}\mathbf{B}/\mathrm{B}^2$ flows towards the x-line, rather than away from it, occur at some locations.
2. The $\mathbf{E}\mathrm{X}\mathbf{B}/\mathrm{B}^2$ flow in the normally ignored Y-direction was far from zero, being as large as several hundred km/sec.
3. There were regions within the magnetopause where electromagnetic energy may have been generated rather than dissipated (in the normal incidence frame tied to the magnetopause).

4. Significant dissipation of electromagnetic energy can occur inside the magnetopause without an electron diffusion region, parallel electric fields, or the electrons being decoupled from the magnetic field.

It is emphasized that these properties are consequences of the Hall MHD and guide electric and magnetic fields in the absence of any additional non-MHD processes.

I. INTRODUCTION

Magnetic field reconnection is a process that both converts magnetic energy to particle energy and that modifies the magnetic field topology by connecting previously independent magnetic field lines. It occurs in laboratory plasmas as well as on the sun and other astrophysical objects, and it is the primary mechanism for providing energy to the plasma in the terrestrial magnetosphere. The microphysics of the reconnection process are beginning to be studied in the lab, by computer simulations and in the magnetosphere, with data from satellites.

Two-dimensional static models of reconnection in the absence of guide fields show the presence of a Hall MHD electric field pointing towards the magnetopause from both sides and a Hall magnetic field component tangential to the magnetopause surface[2,3,4,5,6]. A Polar satellite magnetopause crossing in the vicinity of the sub-solar point, on April 1, 2001[1], also revealed these Hall MHD fields while the magnetic field changed from 80 nT southward in the magnetosheath to 80 nT northward in the magnetosphere. The ions

were decoupled from the magnetic field within the six-ion-skin-depth width of the crossing and the Hall MHD fields were in quantitative agreement with computer simulations. It is emphasized that this is an almost unique diffusion region crossing in the database of ~1000 crossings, which may be due to its close proximity to the x-line as well as to the near-equality of the plasma density and $|B_Z|$ in the asymptotic regions.

II. THE MODEL

Even with its many expected features, the April 1 crossing also displayed unexpected properties. One such set of properties is displayed in Fig.1, which gives the three components of $\mathbf{EXB}/B^2$ measured during the magnetopause crossing of interest. The coordinate system of this figure is fixed to the magnetopause with the magnetosheath plasma incident on the magnetopause in the normal direction. X is in the maximum (minimum) variance direction of the electric (magnetic) field, pointing approximately sunward, and Z in the minimum (maximum) variance direction of the electric (magnetic) field, pointing approximately northward in the ecliptic-normal direction. Each of the panels contains three curves which give the measured quantity and the extreme values of that quantity that are achievable with uncertainties in the electric field components of ±1 mV/m, and in the magnetic field components of ±2 nT. Thus, the spread between the curves is an overestimate of the uncertainty in the measurements. In this plot, time runs from right to left, placing the magnetosphere at the left of the plot and the magnetosheath at the right. Near 0547:08 in Fig. 1, the uncertainties in the flow components are large because the magnetic field decreased to nearly zero. Otherwise, the flows were well

measured so the following general features of the flow cannot be explained as due to experimental error:

- $(\mathbf{EXB}/B^2)_X$ was generally negative near the magnetosheath, at the right of the plot, and positive near the magnetosphere near the left end of the plot, in agreement with the expected flow towards the magnetopause from both sides. However, these flows were small compared to those in the Y- and Z-directions. Thus, the X-component of flow will be small compared to the other components in the model and plots that are developed below.

- $(\mathbf{EXB}/B^2)_Y$ was significantly different from zero, was small at the center of the crossing, and was larger on the magnetospheric side of the crossing than on the magnetosheath side. This large, non-zero flow component requires that any model for this crossing be three-dimensional and include flows in the Y-direction that are normally assumed to be zero in the cartoon of two-dimensional reconnection.

- $(\mathbf{EXB}/B^2)_Z$ reversed sign from its expected negative value south of the x-line to a positive value near the middle of the crossing, and this component of flow was larger on the magnetosheath side of the crossing than on the magnetospheric side. Thus, post-reconnection flow towards rather than away from the X-line was observed at some locations.

In the following discussion, the measured fields will be modeled analytically without invoking additional non-MHD physics beyond the Hall effect, in order to understand to what extent the peculiar properties of the **EXB**/B^2 flows may be understood within the context of a Hall MHD magnetopause. It is assumed that the spacecraft passed through a static magnetopause at a constant velocity in the normal direction, that X/X_0 in Fig. 2 runs from –1 at the magnetosphere to +1 at the magnetosheath, that the variations of the Hall MHD fields across the magnetopause are sinusoidal, and that B_Z varies linearly across the magnetopause. With these assumptions, the smoothed, measured, B_X, B_Y, B_Z, and E_X are fit in Fig. 2 by the model values (which are italicized)

$$B_X = B_N \tag{1a}$$

$$B_Y = B_G + B_0 \sin(\pi X/X_0+\varphi) \tag{1b}$$

$$B_Z = -B_A X/X_0 \tag{1c}$$

$$E_X = -E_0 \sin(\pi X/X_0+\varphi) - E_G \tag{1d}$$

where

B_N = Normal magnetic field = 5 nT

B_G = Guide magnetic field in the Y-direction = 17 nT

B_0 = Amplitude of the Hall magnetic field = 40 nT

B_A = Amplitude of the Z-component magnetic field = 80 nT

E_0 = Amplitude of the Hall electric field = 18 mV/m

E_G = Guide electric field in the X-direction = 3 mV/m

φ = 15 degrees

To complete the definition of the model fields along the spacecraft trajectory, it is assumed that both E_Z and the parallel electric field are zero. With these constraints,

$$E_Y = -E_X B_X / B_Y \quad (2a)$$

$$E_Z = 0 \quad (2b)$$

Equation 2a is shown to be consistent with the experimental data by plotting the measured E_Y and the measured $-E_X B_X/B_Y$ in Fig. 3. Their general agreement attests to the fact that the measured parallel electric field was zero within experimental error through the portions of the crossing discussed in this paper. Their not-exact agreement is due in large measure to the fact that the experimental E_Z was not exactly zero. The regions of zero data in the dashed curve of Fig. 3 occur where the magnitude of B_Y was less than 12 nT and E_Z was not equal to zero, hence where $-E_X B_X/B_Y$ became unrealistically large.

Given the analytical expressions for the electric and magnetic fields along the spacecraft trajectory, one may compute the components of $\boldsymbol{EXB}/B^2$ and compare them with the smoothed, measured flows, as is done in Fig. 4. Because the measured flows are well explained in terms of the model fields, it is necessary to understand what properties of the model fields contribute to the facts that the post-reconnection flow is sometimes toward the X-line and that the Y-component of flow is non-zero. From the model,

$$(\boldsymbol{EXB}/B^2)_Z = (E_X B_Y + E_X B_X^2/B_Y)/B^2 = (E_X/B_Y)(B_X^2 + B_Y^2)/(B_X^2 + B_Y^2 + B_Z^2) \quad (3)$$

This expression can only be positive if E_X and B_Y have the same sign, and, from equations (1), this can happen only if $\sin(\pi X/X_0+\varphi) < 0$. For this case, the signs of both E_X and B_Y are positive if

$$E_0 \,|\sin(\pi X/X_0+\varphi)| > E_G \quad (4a)$$

and

$$B_G > B_0 \,|\sin(\pi X/X_0+\varphi)| \quad (4b)$$

Both E_X and B_Y are negative if

$$E_G > E_0 \,|\sin(\pi X/X_0+\varphi)| \quad (5a)$$

and

$$B_0 \,|\sin(\pi X/X_0+\varphi)| > B_G \quad (5b)$$

For the parameters that fit the magnetopause crossing of interest, the range of values for which $(\boldsymbol{EXB}/B^2)_Z > 0$ is

$$-0.22 > \sin(\pi X/X_0+\varphi) > -0.43 \quad (6)$$

From equations (4) and (5), the condition required for the post-reconnection $\boldsymbol{EXB}/B^2$ flow to be towards the X-line is the existence of Hall MHD electric and magnetic fields in the presence of either or both the guide electric and/or magnetic field.

Similarly,

$$(\boldsymbol{EXB}/B^2)_Y = -E_X B_Z /B^2 \qquad (7)$$

The requirement that this flow component be different from zero is the existence of the Hall MHD E_X at the location of a non-zero B_Z. Thus, the magnetopause must have a three-dimensional flow structure in the presence of Hall MHD physics.

One may consider what the $\boldsymbol{EXB}/B^2$ flow would be at other Z-distances within the magnetopause. At locations north of the X-line, the normal magnetic field component and the Hall component of B_Y change sign. If it is assumed that the B_Y guide field, B_G, also changes sign, then the values of the X- and Y-components of the model magnetic field north of the X-line are the negatives of those south of the X-line, so $(\boldsymbol{EXB}/B^2)_Z$ has the opposite sign north of the X-line. However, $(\boldsymbol{EXB}/B^2)_X$ and $(\boldsymbol{EXB}/B^2)_Y$ would be the same north and south of the X-line.

There is no physical reason why the guide magnetic field should depend on the relative location north or south of the X-line. In fact, the more reasonable assumption is that this field is imposed externally, so it varies in the same way that B_Y varies with Z in

the magnetosheath. This means that the model B_G at locations other than that of the satellite is arbitrary. To consider how the magnetopause might look as a function of X and Z, it will be assumed that B_G is constant, independent of Z. A linear dependence on Z of B_N and B_0 will be assumed. With these assumptions, equations (1) and (2) become

$$B_X = -B_N Z/Z_0 \tag{8a}$$

$$B_Y = B_G - B_0 (Z/Z_0) \sin(\pi X/X_0+\varphi) \tag{8b}$$

$$B_Z = -B_A X/X_0 \tag{8c}$$

$$E_X = -E_0 \sin(\pi X/X_0+\varphi) - E_G \tag{8d}$$

$$E_Y = -E_X B_X/B_Y \tag{8e}$$

$$E_Z = 0 \tag{8f}$$

where Z/Z0 varies from –1 at the location of the satellite crossing to +1 at a similar distance north of the X-line.

The consequences of requiring that this model satisfy Maxwell's equations are next considered. Because div**E** and curl**B** are non-zero, the plasma must provide charge densities and currents whose magnitudes may be calculated from the field model. As seen from the model equations, div**B** = 0. Because E_Y depends on both X and Z, the requirement of a static magnetopause (curl**E** = 0) necessitates that both E_X and E_Z vary in the Y-direction. This is further evidence of the three-dimensional character of the magnetopause.

In the left panel of Fig. 5, the $\boldsymbol{EXB}/B^2$ flow in the X-Z plane, as computed from equations 8, is given. As expected from the earlier discussion, the flow into the magnetopause across the $X/X_0 = \pm 1$ boundaries is small compared to the other component of the flow. The flow north (south) of the X-line is generally northward (southward) with regions of reversed flow in each half of the plane. Vorticies in the flow are present and the spatial variation of the flow is significant.

In the right panel of Fig. 5, the flow is plotted from equations 8 under the assumption that the guide fields, B_G and E_G, are zero. Under this assumption, the flow becomes that which is expected in static, two-dimensional models without guide fields. Namely, the flow is inward from the left and right and outward, as a jet, above and below the X-line. This is further proof that the complex flow with regions of post-reconnection flow towards the X-line are consequences of Hall MHD physics in the presence of guide fields.

In the left panel of Fig. 6, contours of $(\boldsymbol{EXB}/B^2)_Y$ are presented. The flow is generally in the –Y direction and is as large as 1000 km/sec. It is again emphasized that this non-zero flow is extremely different from the absence of Y-directed flow in conventional magnetopause models, and that the complexity of the flow is a natural consequence of the Hall MHD physics in the presence of guide fields.

In the right panel of Fig. 6, contours of $(\boldsymbol{EXB}/B^2)_Y$ are presented for the case that the guide fields, B_G and E_G, are zero. While the flow is symmetric in this case, it remains non-zero because of the Hall MHD electric field (see equation 7).

The current density may be calculated from the curl of the model magnetic field and dotted into the model electric field to produce the contour plots of $\mathbf{j}\cdot\mathbf{E}$ given in the left panel of Fig. 7. In this figure, X_0 = 300 km and Z_0 is approximately X_0 times the ratio of the asymptotic magnetic field to the normal magnetic field[7], which is $300B_A/B_N$ = 4800 km. Surprisingly, the electromagnetic energy dissipation is a minimum at the center of the magnetopause. It varies in space from about –1 to +1 watts/km^3.

As a result of the Hall MHD physics, electromagnetic energy may be generated as well as dissipated within the magnetopause (in the normal incidence frame tied to the magnetopause). In the magnetospheric (magnetosheath) side of the magnetopause, the Hall MHD B_Y has $\delta B_Y/\delta Z>0$ ($\delta B_Y/\delta Z<0$). This produces a negative (positive) current in the X-direction. This current, multiplied by the positive (negative) Hall MHD E_X, results in a negative component of $\mathbf{j}\cdot\mathbf{E}$ in both halves of the magnetopause. This component can exceed the others to cause a net generation of electromagnetic energy in some regions, as is evidenced in the left panel of Fig. 7.

The average value of $\mathbf{j}\cdot\mathbf{E}$ over the surface of the left panel of Fig. 7 is about +0.05 watts/km^3. Because this is sufficient power to accelerate 10^8 ions/cm^2/sec to several kilovolts along the Z-axis, Hall MHD physics could suffice to produce the required

magnetic energy conversion without an electron diffusion region, parallel electric fields, decoupling of electrons from the magnetic field, etc.

In the right panel of Fig. 7, **j**•**E** is given for the case that the guide fields are zero. In this case, the electromagnetic energy dissipation is relatively constant at about 0.4 watts/km^3.

It is emphasized that the detailed features exhibited in Figs. 5, 6, and 7 are model dependent, so they should not be interpreted quantitatively. However, the general results derived from the Hall MHD physics in the model are valid. These are that the $\boldsymbol{EXB}/B^2$ flow in the X-Z plane and the associated Poynting flux may be complex with post-reconnection flows towards the X-line at some locations, that a large and complex $\boldsymbol{EXB}/B^2$ flow in the Y-direction is expected, and that significant electromagnetic energy may be dissipated within the magnetopause in regions where electrons are not decoupled from the magnetic field.

REFERENCES

[1]F.S. Mozer, S.D. Bale, and T.D. Phan, Phys. Rev. Lett., **89**, 015002, 2002.

[2]B. U. Ö. Sonnerup, in *Solar System Plasma Physics*, vol. III (ed L.T. Lanzerotti, C.F. Kennel, and E.N. Parker) 45-108 (North-Holland, New York, (1979)

[3]M. Hesse et al., *J. Geophys. Res.*, **106,** 3721 (2001)

[4]M. A. Shay et al, *J. Geophys. Res.*, **106,** 3759, (2001)

[5]Z. W. Ma and A. Bhattacharjee, *J. Geophys. Res.*, **106,** 3773 (2001).

[6]P. L. Pritchett, *J. Geophys. Res.*, **106,** 3783 (2001)

[7]B.U.O. Sonnerup, G. Paschmann, I Papamastorakis, N. Sckopke, G. Haerendel, S.J. Bame, J.R. Asbridge, J.T. Gosling, and C.T. Russell, J. Geophys. Res., **86**, 10049, 1981.

FIGURE CAPTIONS

Fig. 1. Measured components of $\mathbf{E}\mathrm{X}\mathbf{B}/\mathrm{B}^2$ in the minimum variance coordinate system fixed to the magnetopause. Note that time runs backwards such that the magnetosphere is at the left boundary of the plots and the magnetosheath is at the right boundary.

Fig. 2. Comparison of smoothed, measured, magnetic field components and E_X (the solid curves) with model fields described by equations 1 (the dashed curves).

Fig. 3. Comparison of the measured Y-component of the electric field (solid curve) with $-E_X B_X/B_Y$ (the dashed curve). Note that time runs backwards such that the magnetosphere is at the left boundary of the plot and the magnetosheath is at the right boundary.

Fig. 4. Comparison of the smoothed, measured, components of $\mathbf{E}\mathrm{X}\mathbf{B}/\mathrm{B}^2$ (the solid curves) with the model values (the dashed curves).

Fig. 5. The model **E**X**B**/B^2 flow in the X-Z plane. The left panel includes the guide fields B_Y = 17 nT and E_X = 3 mV/m. The right panel assumes that these guide fields are zero.

Fig. 6. The Y-component of **E**X**B**/B^2 in the X-Z plane. The left panel includes the guide fields B_Y = 17 nT and E_X = 3 mV/m. The right panel assumes that these guide fields are zero.

Fig. 7. Electromagnetic energy dissipation in the X-Z plane. The left panel includes the guide fields B_Y = 17 nT and E_X = 3 mV/m. The right panel assumes that these guide fields are zero.

THE COMPLEX, THREE-DIMENSIONAL MAGNETOPAUSE

F.S. Mozer, T.D. Phan, and S.D. Bale

Physics Department and Space Sciences Laboratory

University of California, Berkeley, CA. 94720

ABSTRACT

Electric and magnetic fields observed in a one-of-a-kind example of a Polar satellite magnetopause crossing[1] are consistent with static guide magnetic and electric fields, Hall MHD electric and magnetic fields, and a Z-component magnetic field that varied from –80 nT to +80 nT across the magnetopause. In spite of this excellent agreement with simulations, other features of the data were unanticipated. We develop an empirical model based on these measured fields and the assumption that the parallel electric field was zero, to explain such features by showing that:

1. Post-reconnection $\mathbf{E}\mathrm{X}\mathbf{B}/\mathrm{B}^2$ flows towards the x-line, rather than away from it, occur at some locations.
2. The $\mathbf{E}\mathrm{X}\mathbf{B}/\mathrm{B}^2$ flow in the normally ignored Y-direction was far from zero, being as large as several hundred km/sec.
3. There were regions within the magnetopause where electromagnetic energy may have been generated rather than dissipated (in the normal incidence frame tied to the magnetopause).

4. Significant dissipation of electromagnetic energy can occur inside the magnetopause without an electron diffusion region, parallel electric fields, or the electrons being decoupled from the magnetic field.

It is emphasized that these properties are consequences of the Hall MHD and guide electric and magnetic fields in the absence of any additional non-MHD processes.

I. INTRODUCTION

Magnetic field reconnection is a process that both converts magnetic energy to particle energy and that modifies the magnetic field topology by connecting previously independent magnetic field lines. It occurs in laboratory plasmas as well as on the sun and other astrophysical objects, and it is the primary mechanism for providing energy to the plasma in the terrestrial magnetosphere. The microphysics of the reconnection process are beginning to be studied in the lab, by computer simulations and in the magnetosphere, with data from satellites.

Two-dimensional static models of reconnection in the absence of guide fields show the presence of a Hall MHD electric field pointing towards the magnetopause from both sides and a Hall magnetic field component tangential to the magnetopause surface[2,3,4,5,6]. A Polar satellite magnetopause crossing in the vicinity of the sub-solar point, on April 1, 2001[1], also revealed these Hall MHD fields while the magnetic field changed from 80 nT southward in the magnetosheath to 80 nT northward in the magnetosphere. The ions

were decoupled from the magnetic field within the six-ion-skin-depth width of the crossing and the Hall MHD fields were in quantitative agreement with computer simulations. It is emphasized that this is an almost unique diffusion region crossing in the database of ~1000 crossings, which may be due to its close proximity to the x-line as well as to the near-equality of the plasma density and $|B_Z|$ in the asymptotic regions.

II. THE MODEL

Even with its many expected features, the April 1 crossing also displayed unexpected properties. One such set of properties is displayed in Fig.1, which gives the three components of $\mathbf{EXB}/B^2$ measured during the magnetopause crossing of interest. The coordinate system of this figure is fixed to the magnetopause with the magnetosheath plasma incident on the magnetopause in the normal direction. X is in the maximum (minimum) variance direction of the electric (magnetic) field, pointing approximately sunward, and Z in the minimum (maximum) variance direction of the electric (magnetic) field, pointing approximately northward in the ecliptic-normal direction. Each of the panels contains three curves which give the measured quantity and the extreme values of that quantity that are achievable with uncertainties in the electric field components of ±1 mV/m, and in the magnetic field components of ±2 nT. Thus, the spread between the curves is an overestimate of the uncertainty in the measurements. In this plot, time runs from right to left, placing the magnetosphere at the left of the plot and the magnetosheath at the right. Near 0547:08 in Fig. 1, the uncertainties in the flow components are large because the magnetic field decreased to nearly zero. Otherwise, the flows were well

measured so the following general features of the flow cannot be explained as due to experimental error:

- $(\mathbf{EXB}/B^2)_X$ was generally negative near the magnetosheath, at the right of the plot, and positive near the magnetosphere near the left end of the plot, in agreement with the expected flow towards the magnetopause from both sides. However, these flows were small compared to those in the Y- and Z-directions. Thus, the X-component of flow will be small compared to the other components in the model and plots that are developed below.

- $(\mathbf{EXB}/B^2)_Y$ was significantly different from zero, was small at the center of the crossing, and was larger on the magnetospheric side of the crossing than on the magnetosheath side. This large, non-zero flow component requires that any model for this crossing be three-dimensional and include flows in the Y-direction that are normally assumed to be zero in the cartoon of two-dimensional reconnection.

- $(\mathbf{EXB}/B^2)_Z$ reversed sign from its expected negative value south of the x-line to a positive value near the middle of the crossing, and this component of flow was larger on the magnetosheath side of the crossing than on the magnetospheric side. Thus, post-reconnection flow towards rather than away from the X-line was observed at some locations.

In the following discussion, the measured fields will be modeled analytically without invoking additional non-MHD physics beyond the Hall effect, in order to understand to what extent the peculiar properties of the **EXB**/B^2 flows may be understood within the context of a Hall MHD magnetopause. It is assumed that the spacecraft passed through a static magnetopause at a constant velocity in the normal direction, that X/X_0 in Fig. 2 runs from –1 at the magnetosphere to +1 at the magnetosheath, that the variations of the Hall MHD fields across the magnetopause are sinusoidal, and that B_Z varies linearly across the magnetopause. With these assumptions, the smoothed, measured, B_X, B_Y, B_Z, and E_X are fit in Fig. 2 by the model values (which are italicized)

$$B_X = B_N \tag{1a}$$

$$B_Y = B_G + B_0 \sin(\pi X/X_0+\varphi) \tag{1b}$$

$$B_Z = -B_A X/X_0 \tag{1c}$$

$$E_X = -E_0 \sin(\pi X/X_0+\varphi) - E_G \tag{1d}$$

where

B_N = Normal magnetic field = 5 nT

B_G = Guide magnetic field in the Y-direction = 17 nT

B_0 = Amplitude of the Hall magnetic field = 40 nT

B_A = Amplitude of the Z-component magnetic field = 80 nT

E_0 = Amplitude of the Hall electric field = 18 mV/m

E_G = Guide electric field in the X-direction = 3 mV/m

φ = 15 degrees

To complete the definition of the model fields along the spacecraft trajectory, it is assumed that both E_Z and the parallel electric field are zero. With these constraints,

$$E_Y = -E_X B_X / B_Y \quad (2a)$$

$$E_Z = 0 \quad (2b)$$

Equation 2a is shown to be consistent with the experimental data by plotting the measured E_Y and the measured $-E_X B_X/B_Y$ in Fig. 3. Their general agreement attests to the fact that the measured parallel electric field was zero within experimental error through the portions of the crossing discussed in this paper. Their not-exact agreement is due in large measure to the fact that the experimental E_Z was not exactly zero. The regions of zero data in the dashed curve of Fig. 3 occur where the magnitude of B_Y was less than 12 nT and E_Z was not equal to zero, hence where $-E_X B_X/B_Y$ became unrealistically large.

Given the analytical expressions for the electric and magnetic fields along the spacecraft trajectory, one may compute the components of $\boldsymbol{EXB}/B^2$ and compare them with the smoothed, measured flows, as is done in Fig. 4. Because the measured flows are well explained in terms of the model fields, it is necessary to understand what properties of the model fields contribute to the facts that the post-reconnection flow is sometimes toward the X-line and that the Y-component of flow is non-zero. From the model,

$$(\boldsymbol{EXB}/B^2)_Z = (E_X B_Y + E_X B_X^2/B_Y)/B^2 = (E_X/B_Y)(B_X^2 + B_Y^2)/(B_X^2 + B_Y^2 + B_Z^2) \quad (3)$$

This expression can only be positive if E_X and B_Y have the same sign, and, from equations (1), this can happen only if $\sin(\pi X/X_0+\varphi) < 0$. For this case, the signs of both E_X and B_Y are positive if

$$E_0 \,|\sin(\pi X/X_0+\varphi)| > E_G \quad (4a)$$

and

$$B_G > B_0 \,|\sin(\pi X/X_0+\varphi)| \quad (4b)$$

Both E_X and B_Y are negative if

$$E_G > E_0 \,|\sin(\pi X/X_0+\varphi)| \quad (5a)$$

and

$$B_0 \,|\sin(\pi X/X_0+\varphi)| > B_G \quad (5b)$$

For the parameters that fit the magnetopause crossing of interest, the range of values for which $(\boldsymbol{EXB}/B^2)_Z > 0$ is

$$-0.22 > \sin(\pi X/X_0+\varphi) > -0.43 \quad (6)$$

From equations (4) and (5), the condition required for the post-reconnection $\boldsymbol{EXB}/B^2$ flow to be towards the X-line is the existence of Hall MHD electric and magnetic fields in the presence of either or both the guide electric and/or magnetic field.

Similarly,

$$(\boldsymbol{EXB}/B^2)_Y = -E_X B_Z /B^2 \qquad (7)$$

The requirement that this flow component be different from zero is the existence of the Hall MHD E_X at the location of a non-zero B_Z. Thus, the magnetopause must have a three-dimensional flow structure in the presence of Hall MHD physics.

One may consider what the $\boldsymbol{EXB}/B^2$ flow would be at other Z-distances within the magnetopause. At locations north of the X-line, the normal magnetic field component and the Hall component of B_Y change sign. If it is assumed that the B_Y guide field, B_G, also changes sign, then the values of the X- and Y-components of the model magnetic field north of the X-line are the negatives of those south of the X-line, so $(\boldsymbol{EXB}/B^2)_Z$ has the opposite sign north of the X-line. However, $(\boldsymbol{EXB}/B^2)_X$ and $(\boldsymbol{EXB}/B^2)_Y$ would be the same north and south of the X-line.

There is no physical reason why the guide magnetic field should depend on the relative location north or south of the X-line. In fact, the more reasonable assumption is that this field is imposed externally, so it varies in the same way that B_Y varies with Z in

the magnetosheath. This means that the model B_G at locations other than that of the satellite is arbitrary. To consider how the magnetopause might look as a function of X and Z, it will be assumed that B_G is constant, independent of Z. A linear dependence on Z of B_N and B_0 will be assumed. With these assumptions, equations (1) and (2) become

$$B_X = -B_N Z/Z_0 \tag{8a}$$

$$B_Y = B_G - B_0 (Z/Z_0) \sin(\pi X/X_0+\varphi) \tag{8b}$$

$$B_Z = -B_A X/X_0 \tag{8c}$$

$$E_X = -E_0 \sin(\pi X/X_0+\varphi) - E_G \tag{8d}$$

$$E_Y = -E_X B_X/B_Y \tag{8e}$$

$$E_Z = 0 \tag{8f}$$

where Z/Z0 varies from –1 at the location of the satellite crossing to +1 at a similar distance north of the X-line.

The consequences of requiring that this model satisfy Maxwell's equations are next considered. Because div**E** and curl**B** are non-zero, the plasma must provide charge densities and currents whose magnitudes may be calculated from the field model. As seen from the model equations, div**B** = 0. Because E_Y depends on both X and Z, the requirement of a static magnetopause (curl**E** = 0) necessitates that both E_X and E_Z vary in the Y-direction. This is further evidence of the three-dimensional character of the magnetopause.

In the left panel of Fig. 5, the $\boldsymbol{EXB}/B^2$ flow in the X-Z plane, as computed from equations 8, is given. As expected from the earlier discussion, the flow into the magnetopause across the $X/X_0 = \pm 1$ boundaries is small compared to the other component of the flow. The flow north (south) of the X-line is generally northward (southward) with regions of reversed flow in each half of the plane. Vorticies in the flow are present and the spatial variation of the flow is significant.

In the right panel of Fig. 5, the flow is plotted from equations 8 under the assumption that the guide fields, B_G and E_G, are zero. Under this assumption, the flow becomes that which is expected in static, two-dimensional models without guide fields. Namely, the flow is inward from the left and right and outward, as a jet, above and below the X-line. This is further proof that the complex flow with regions of post-reconnection flow towards the X-line are consequences of Hall MHD physics in the presence of guide fields.

In the left panel of Fig. 6, contours of $(\boldsymbol{EXB}/B^2)_Y$ are presented. The flow is generally in the –Y direction and is as large as 1000 km/sec. It is again emphasized that this non-zero flow is extremely different from the absence of Y-directed flow in conventional magnetopause models, and that the complexity of the flow is a natural consequence of the Hall MHD physics in the presence of guide fields.

In the right panel of Fig. 6, contours of $(\boldsymbol{EXB}/B^2)_Y$ are presented for the case that the guide fields, B_G and E_G, are zero. While the flow is symmetric in this case, it remains non-zero because of the Hall MHD electric field (see equation 7).

The current density may be calculated from the curl of the model magnetic field and dotted into the model electric field to produce the contour plots of $\mathbf{j}\cdot\mathbf{E}$ given in the left panel of Fig. 7. In this figure, X_0 = 300 km and Z_0 is approximately X_0 times the ratio of the asymptotic magnetic field to the normal magnetic field[7], which is $300B_A/B_N$ = 4800 km. Surprisingly, the electromagnetic energy dissipation is a minimum at the center of the magnetopause. It varies in space from about –1 to +1 watts/km^3.

As a result of the Hall MHD physics, electromagnetic energy may be generated as well as dissipated within the magnetopause (in the normal incidence frame tied to the magnetopause). In the magnetospheric (magnetosheath) side of the magnetopause, the Hall MHD B_Y has $\delta B_Y/\delta Z>0$ ($\delta B_Y/\delta Z<0$). This produces a negative (positive) current in the X-direction. This current, multiplied by the positive (negative) Hall MHD E_X, results in a negative component of $\mathbf{j}\cdot\mathbf{E}$ in both halves of the magnetopause. This component can exceed the others to cause a net generation of electromagnetic energy in some regions, as is evidenced in the left panel of Fig. 7.

The average value of $\mathbf{j}\cdot\mathbf{E}$ over the surface of the left panel of Fig. 7 is about +0.05 watts/km^3. Because this is sufficient power to accelerate 10^8 ions/cm^2/sec to several kilovolts along the Z-axis, Hall MHD physics could suffice to produce the required

magnetic energy conversion without an electron diffusion region, parallel electric fields, decoupling of electrons from the magnetic field, etc.

In the right panel of Fig. 7, **j**•**E** is given for the case that the guide fields are zero. In this case, the electromagnetic energy dissipation is relatively constant at about 0.4 watts/km^3.

It is emphasized that the detailed features exhibited in Figs. 5, 6, and 7 are model dependent, so they should not be interpreted quantitatively. However, the general results derived from the Hall MHD physics in the model are valid. These are that the $\boldsymbol{EXB}/B^2$ flow in the X-Z plane and the associated Poynting flux may be complex with post-reconnection flows towards the X-line at some locations, that a large and complex $\boldsymbol{EXB}/B^2$ flow in the Y-direction is expected, and that significant electromagnetic energy may be dissipated within the magnetopause in regions where electrons are not decoupled from the magnetic field.

REFERENCES

[1]F.S. Mozer, S.D. Bale, and T.D. Phan, Phys. Rev. Lett., **89**, 015002, 2002.

[2]B. U. Ö. Sonnerup, in *Solar System Plasma Physics*, vol. III (ed L.T. Lanzerotti, C.F. Kennel, and E.N. Parker) 45-108 (North-Holland, New York, (1979)

[3]M. Hesse et al., *J. Geophys. Res.*, **106,** 3721 (2001)

[4]M. A. Shay et al, *J. Geophys. Res.*, **106,** 3759, (2001)

[5]Z. W. Ma and A. Bhattacharjee, *J. Geophys. Res.*, **106,** 3773 (2001).

[6]P. L. Pritchett, *J. Geophys. Res.*, **106,** 3783 (2001)

[7]B.U.O. Sonnerup, G. Paschmann, I Papamastorakis, N. Sckopke, G. Haerendel, S.J. Bame, J.R. Asbridge, J.T. Gosling, and C.T. Russell, J. Geophys. Res., **86**, 10049, 1981.

FIGURE CAPTIONS

Fig. 1. Measured components of $\mathbf{E}\mathrm{X}\mathbf{B}/\mathrm{B}^2$ in the minimum variance coordinate system fixed to the magnetopause. Note that time runs backwards such that the magnetosphere is at the left boundary of the plots and the magnetosheath is at the right boundary.

Fig. 2. Comparison of smoothed, measured, magnetic field components and E_X (the solid curves) with model fields described by equations 1 (the dashed curves).

Fig. 3. Comparison of the measured Y-component of the electric field (solid curve) with $-E_X B_X/B_Y$ (the dashed curve). Note that time runs backwards such that the magnetosphere is at the left boundary of the plot and the magnetosheath is at the right boundary.

Fig. 4. Comparison of the smoothed, measured, components of $\mathbf{E}\mathrm{X}\mathbf{B}/\mathrm{B}^2$ (the solid curves) with the model values (the dashed curves).

Fig. 5. The model **E**X**B**/B^2 flow in the X-Z plane. The left panel includes the guide fields B_Y = 17 nT and E_X = 3 mV/m. The right panel assumes that these guide fields are zero.

Fig. 6. The Y-component of **E**X**B**/B^2 in the X-Z plane. The left panel includes the guide fields B_Y = 17 nT and E_X = 3 mV/m. The right panel assumes that these guide fields are zero.

Fig. 7. Electromagnetic energy dissipation in the X-Z plane. The left panel includes the guide fields B_Y = 17 nT and E_X = 3 mV/m. The right panel assumes that these guide fields are zero.

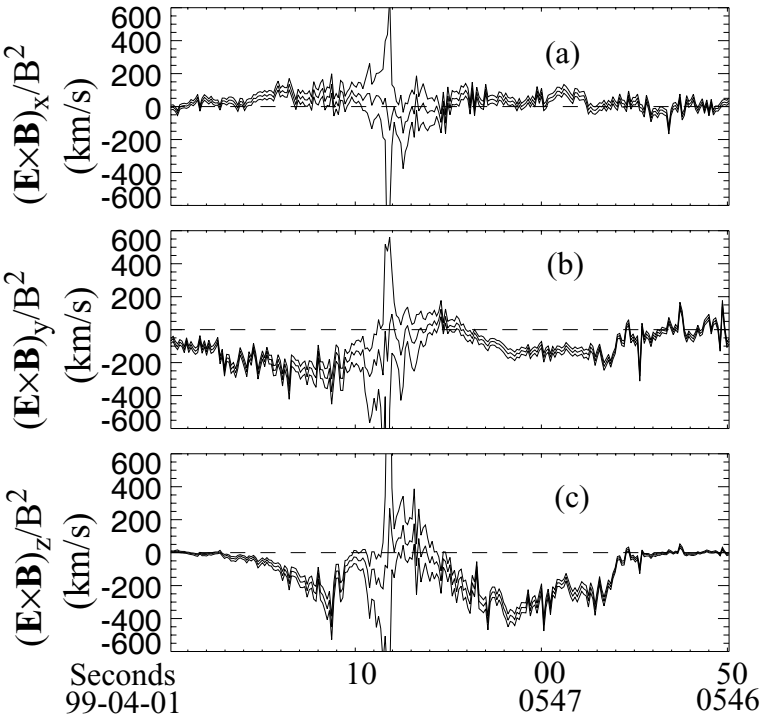
(E×B)x/B2 (km/s)
(E×B)y/B2 (km/s)
(E×B)z/B2 (km/s)
600
400
200
0
-200
-400
-600
(a)
(b)
(c)
Seconds
10
00
50
99-04-01
0547
0546

Figure 1

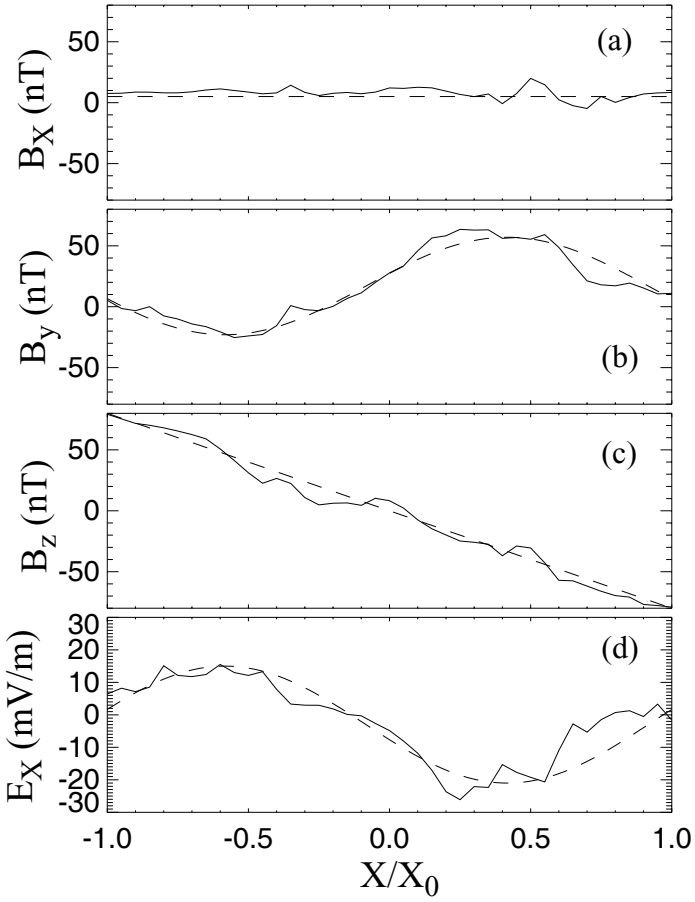
(a)
(b)
(c)
(d)
B_X (nT)
B_y (nT)
B_z (nT)
E_X (mV/m)
50
0
-50
30
20
10
-10
-20
-30
-1.0
-0.5
0.0
0.5
1.0
X/X_0

Figure 2

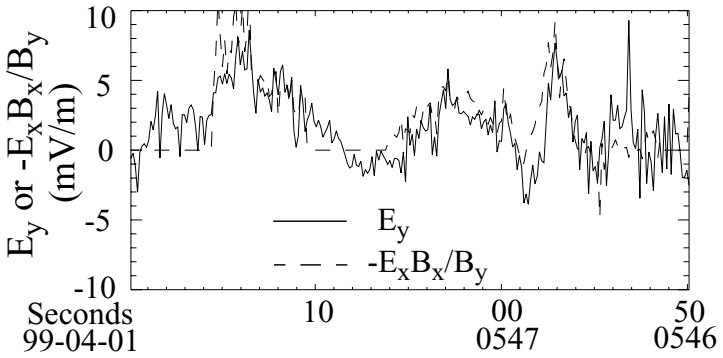
10
5
0
-5
-10
E_y or $-E_xB_x/B_y$ (mV/m)
E_y
$-E_xB_x/B_y$
Seconds
10
00
50
99-04-01
0547
0546

Figure 3

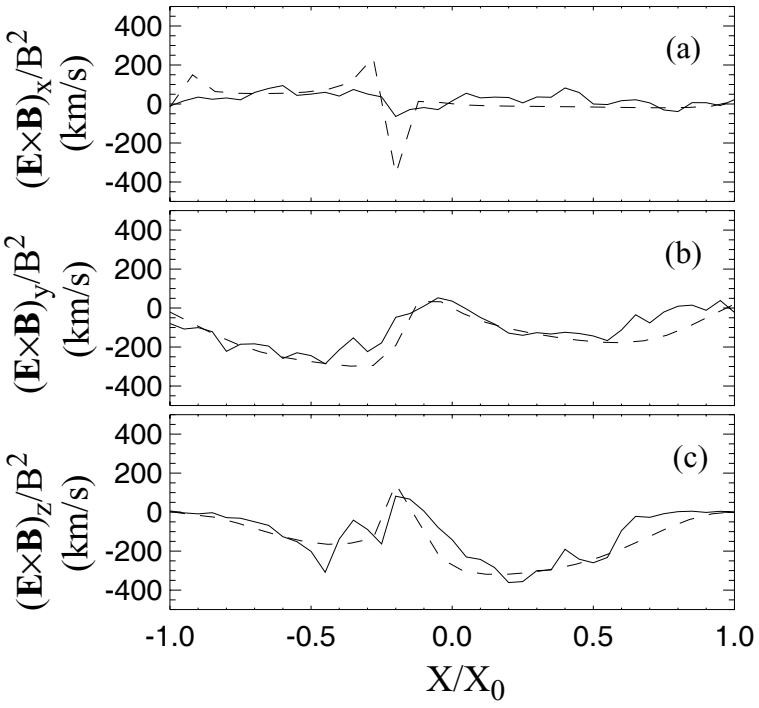
(E×B)x/B2 (km/s)
(E×B)y/B2 (km/s)
(E×B)z/B2 (km/s)
(a)
(b)
(c)
400
200
0
-200
-400
-1.0
-0.5
0.0
0.5
1.0
X/X0

Figure 4

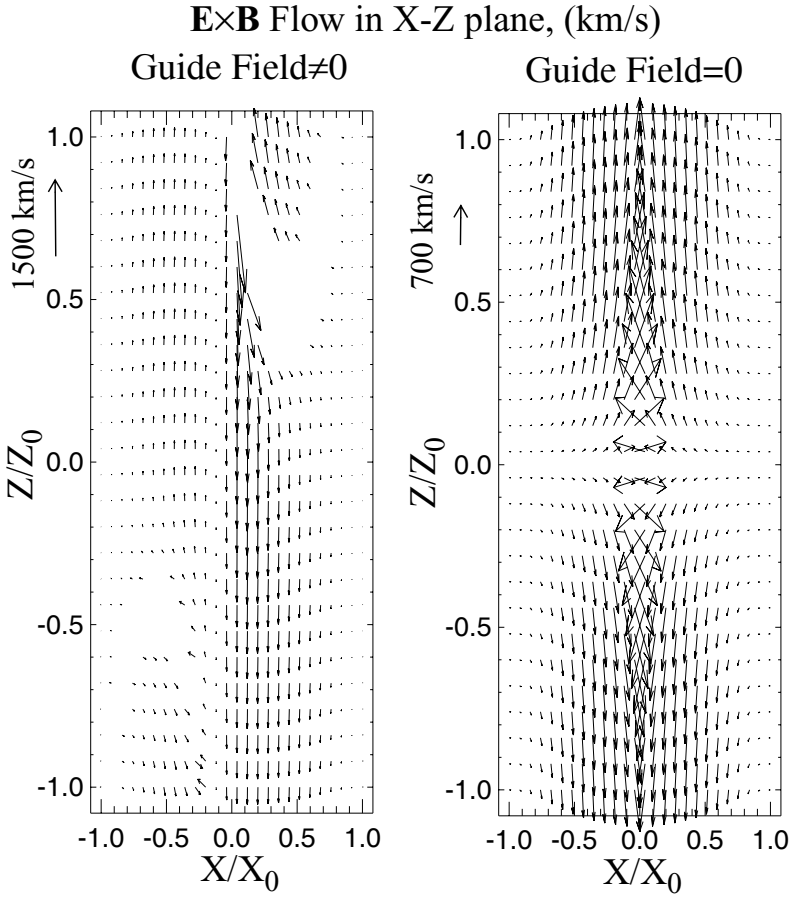
E×**B** Flow in X-Z plane, (km/s)
Guide Field≠0
Guide Field=0
1500 km/s
700 km/s
Z/Z0
X/X0
1.0
0.5
0.0
-0.5
-1.0

Figure 5

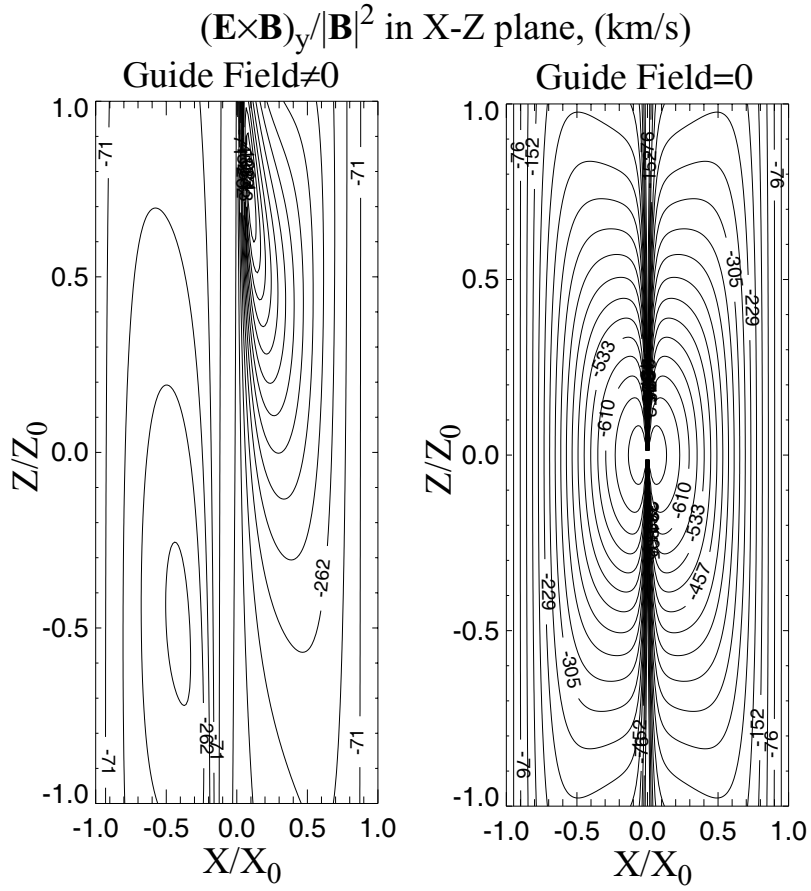
$(\mathbf{E}\times\mathbf{B})_y/|\mathbf{B}|^2$ in X-Z plane, (km/s)
Guide Field≠0
Guide Field=0
Z/Z0
X/X0
1.0
0.5
0.0
-0.5
-1.0
-71
-262
-533
-610
-457
-305
-229
-152
-76

Figure 6

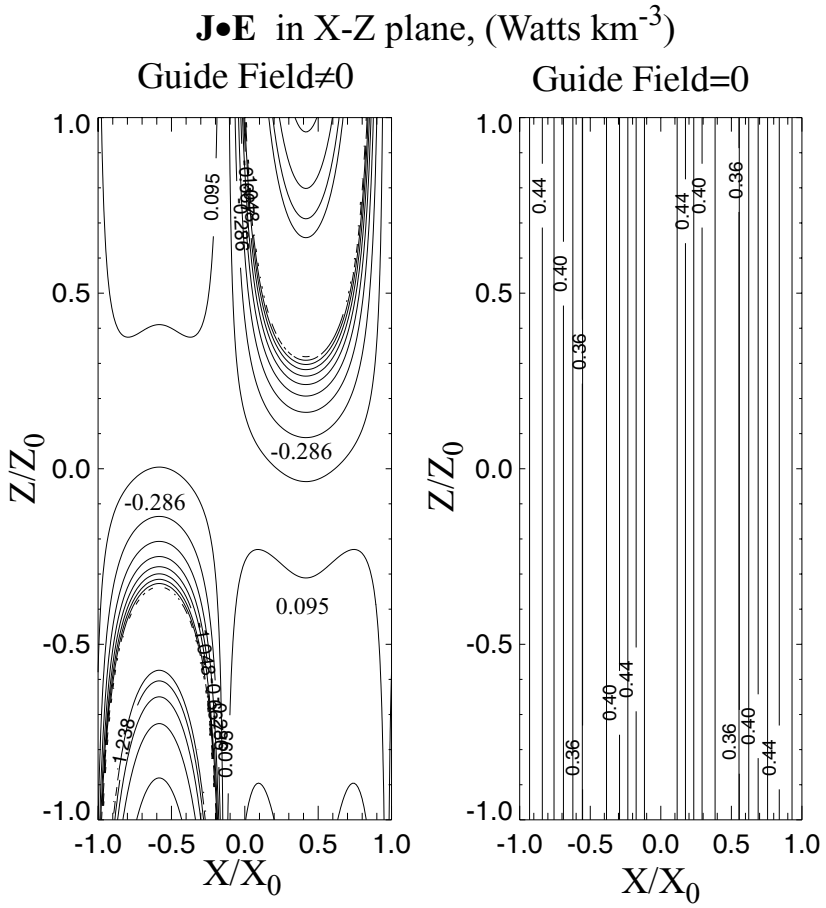
J•E in X-Z plane, (Watts km-3)
Guide Field≠0
Guide Field=0
Z/Z0
X/X0
1.0
0.5
0.0
-0.5
-1.0
-1.0
-0.5
0.0
0.5
1.0
0.095
-0.286
-0.286
0.095
1.238
0.44
0.40
0.36

Figure 7

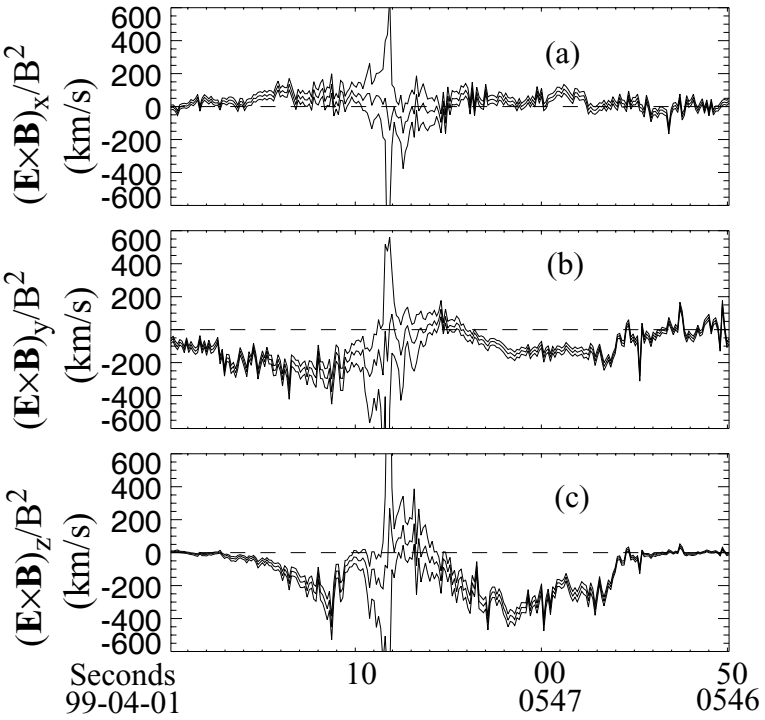
(E×B)x/B2 (km/s)
(E×B)y/B2 (km/s)
(E×B)z/B2 (km/s)
600
400
200
0
-200
-400
-600
(a)
(b)
(c)
Seconds
10
00
50
99-04-01
0547
0546

Figure 1

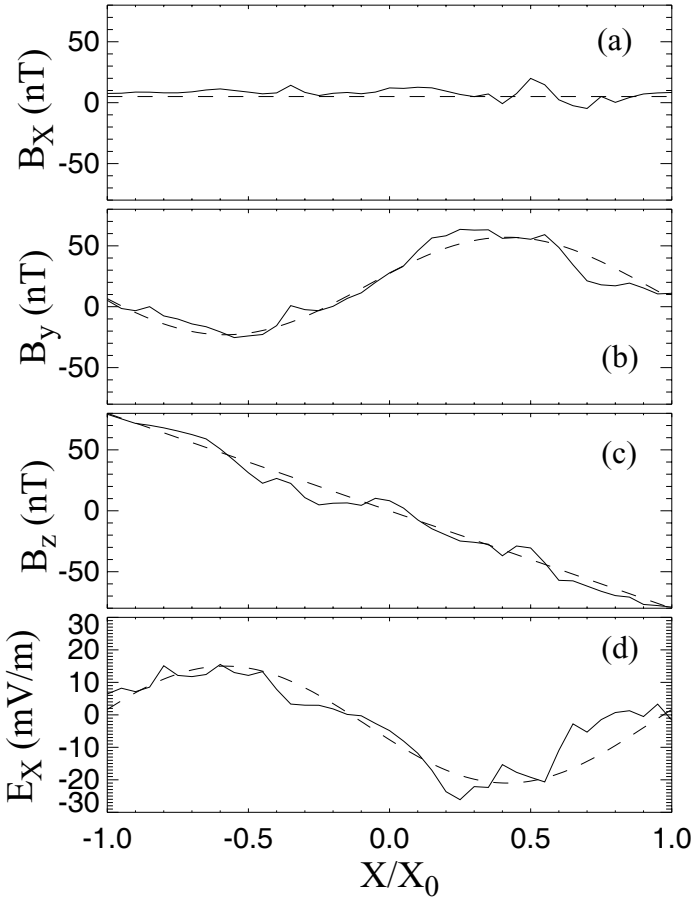
(a)
(b)
(c)
(d)
B_X (nT)
B_y (nT)
B_z (nT)
E_X (mV/m)
50
0
-50
30
20
10
-10
-20
-30
-1.0
-0.5
0.0
0.5
1.0
X/X_0

Figure 2

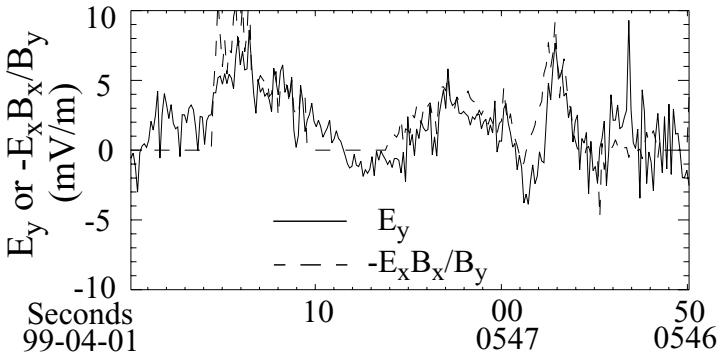
10
5
0
-5
-10
E_y or $-E_xB_x/B_y$ (mV/m)
E_y
$-E_xB_x/B_y$
Seconds
10
00
50
99-04-01
0547
0546

Figure 3

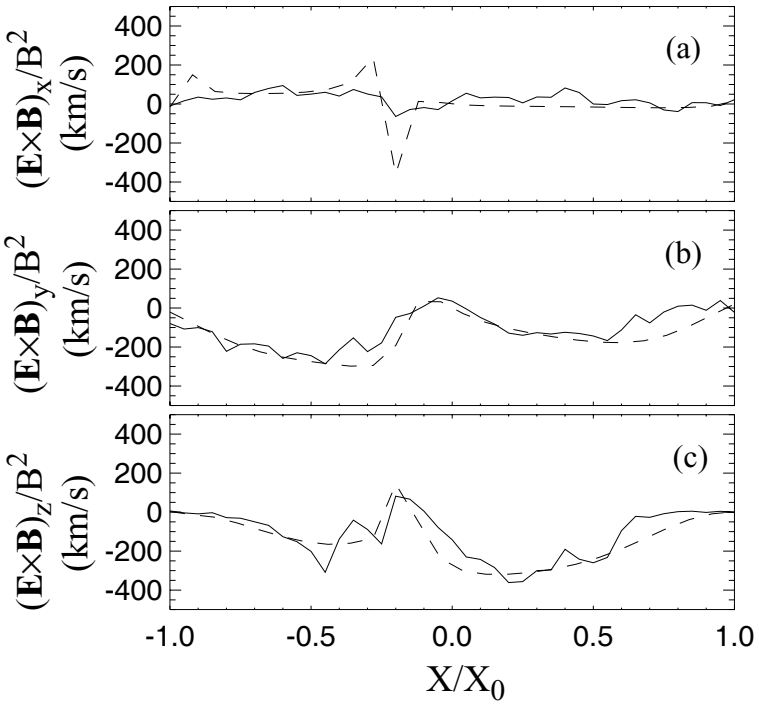
(E×B)x/B2 (km/s)
(E×B)y/B2 (km/s)
(E×B)z/B2 (km/s)
(a)
(b)
(c)
400
200
0
-200
-400
-1.0
-0.5
0.0
0.5
1.0
X/X0

Figure 4

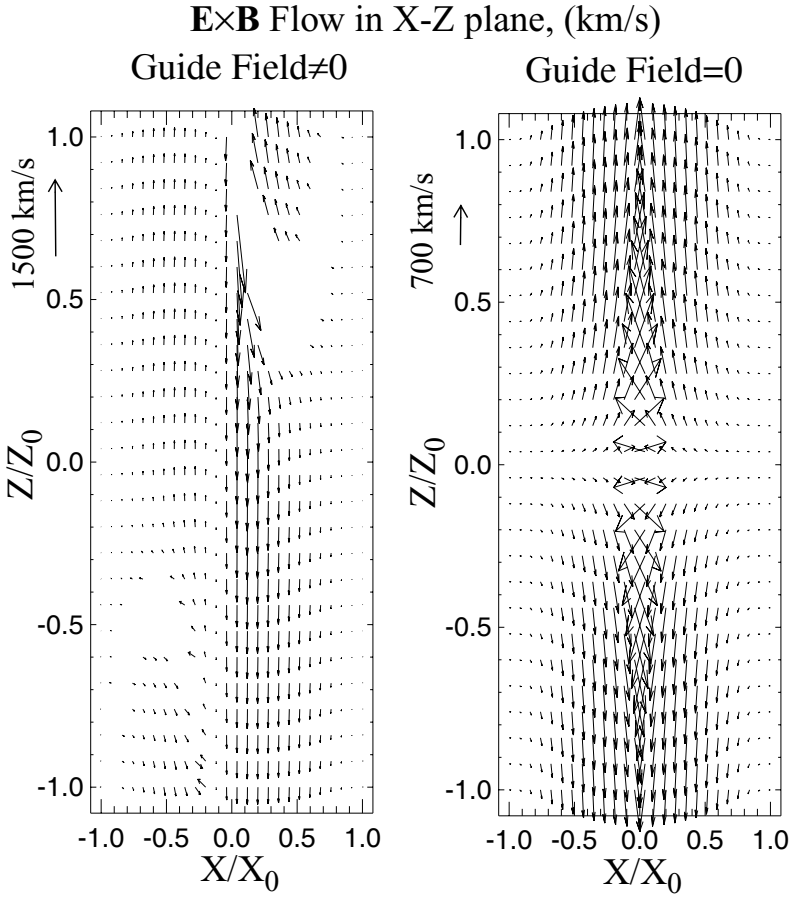
E×**B** Flow in X-Z plane, (km/s)
Guide Field≠0
Guide Field=0
1500 km/s
700 km/s
Z/Z0
X/X0
1.0
0.5
0.0
-0.5
-1.0

Figure 5

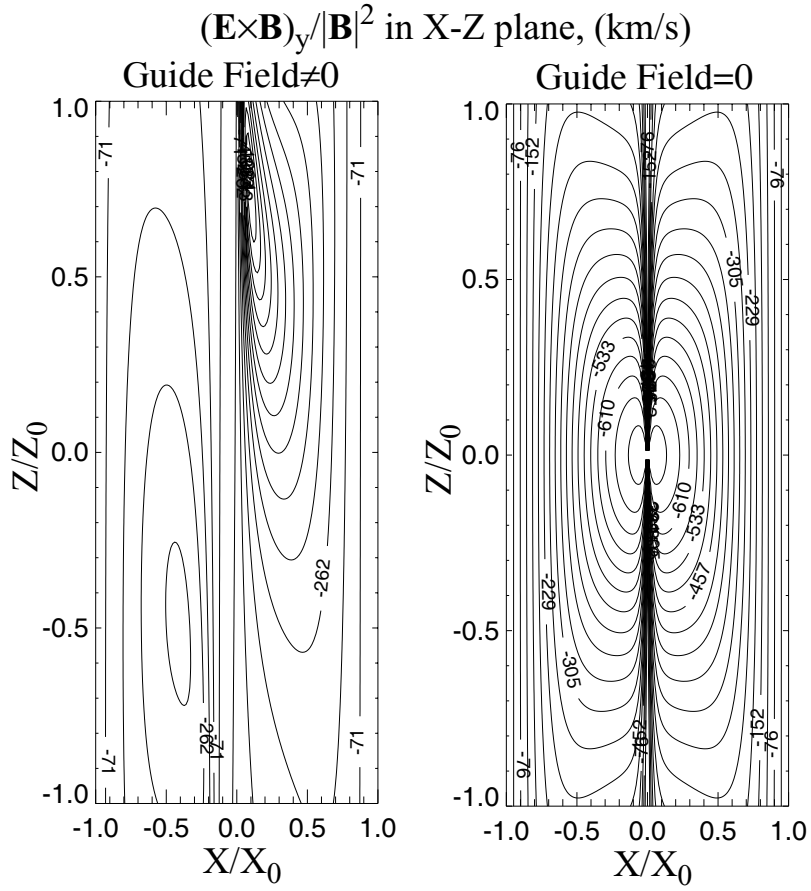
$(\mathbf{E}\times\mathbf{B})_y/|\mathbf{B}|^2$ in X-Z plane, (km/s)
Guide Field≠0
Guide Field=0
Z/Z0
X/X0
1.0
0.5
0.0
-0.5
-1.0
-71
-262
-533
-610
-457
-305
-229
-152
-76

Figure 6